Title: The WOPR family protein Ryp1 is a key regulator of gene expression, development, and virulence in the thermally dimorphic fungal pathogen *Coccidioides posadasii*

M. Alejandra Mandel[1,2]*, Sinem Beyhan[3,4,5]*, Mark Voorhies[3], Lisa F. Shubitz[2], John N. Galgiani[2], Marc J.Orbach[1,2]#, Anita Sil[3]#

*Co-first authors

#Co-corresponding authors

Affiliations:

[1]School of Plant Sciences, University of Arizona, Tucson, AZ 85721, USA

[2]Valley Fever Center for Excellence, The University of Arizona, Tucson, AZ 85724, USA

[3]Department of Microbiology and Immunology, University of California San Francisco, San Francisco, CA 94143, USA

[4]Current address: Department of Infectious Diseases, J. Craig Venter Institute, La Jolla, CA 92037, USA

[5]Current address: Department of Medicine, University of California San Diego, La Jolla, CA 92037, USA

Running title: Ryp1 regulates spherule development and virulence in *C. posadasii*

Keywords: *Coccidioides posadasii*, morphology, virulence, dimorphic fungi

Correspondence: anita.sil@ucsf.edu, orbachmj@arizona.edu

Abstract

Coccidioides spp. are mammalian fungal pathogens endemic to the southwestern US and other desert regions of Mexico, central and South America, with the bulk of US infections occurring in California and Arizona. In the soil, *Coccidioides* grows in a hyphal form that differentiates into 3-5 micron asexual spores (arthroconidia). When arthroconidia are inhaled by mammals they undergo a unique developmental transition from polar hyphal growth to isotropic expansion with multiple rounds of nuclear division, prior to segmentation, forming large spherules filled with endospores. Very little is understood about the molecular basis of spherule formation. Here we characterize the role of the conserved transcription factor Ryp1 in *Coccidioides* development. We show that *Coccidioides* Δ*ryp1* mutants have altered colony morphology under hypha-promoting conditions and are unable to form mature spherules under spherule-promoting conditions. We analyze the transcriptional profile of wild-type and Δ*ryp1* mutant cells under hypha- and spherule-promoting conditions, thereby defining a set of hypha- or spherule-enriched transcripts ("morphology-regulated" genes) that are dependent on Ryp1 for their expression. Forty percent of morphology-regulated expression is Ryp1-dependent, indicating that Ryp1 plays a dual role in both hyphal and spherule development. Ryp1-dependent transcripts include key virulence factors such as SOWgp, which encodes the spherule outer wall glycoprotein. Concordant with its role in spherule development, we find that the Δ*ryp1* mutant is completely avirulent in the mouse model of coccidioidomycosis, indicating that Ryp1-dependent pathways are essential for the ability of *Coccidioides* to cause disease. Vaccination of C57BL/6 mice with live Δ*ryp1* spores does not provide any protection from lethal *C. posadasii* intranasal infection, consistent with our findings that the Δ*ryp1* mutant fails to make mature spherules and likely does not express key antigens required for effective vaccination. Taken together, this work identifies the first transcription factor that drives mature spherulation and virulence in *Coccidioides*.

Author Summary

Coccidioides species, *C. immitis* and *C. posadasii*, are dimorphic fungal pathogens that commonly infect humans in North, Central, and South America, causing the respiratory fungal disease known as Valley Fever. *Coccidioides* grows as hyphae in the soil and differentiates into unique structures called spherules in the mammalian host. Spherules expand and internally divide to form endospores, which are released to facilitate dissemination of the pathogen within the host. The mechanisms underlying spherule differentiation remain largely unknown. In this study, we generated knockout mutants (Δ*ryp1*) of the conserved transcription factor Ryp1 in *C. posadasii* and characterized its role in spherule formation and virulence. We found that Ryp1 is required for the formation of mature spherules and colonization of mouse lungs. Transcriptional profiling of the Δ*ryp1* mutant and the wild-type strain shows that Ryp1 regulates the expression of a subset of the transcripts that are either upregulated in wild-type spherules or in wild-type hyphae. These findings suggest that Ryp1 has a dual role in regulating morphology and virulence under host conditions as well as regulating genes involved in hyphal growth in the environment.

Introduction

Coccidioides spp. are fungal pathogens endemic to California, Arizona, and other desert regions in the Americas [1]. *Coccidioides* infects otherwise healthy individuals when they inhale spores from the soil. The prevalence of *Coccidioides* infection rose 9-fold between 1998 and 2011 and has continued to spike, with incidence now at an all-time high [2]. Elegant observational studies of *Coccidioides* have established its complex life cycle, its disease etiology, and its interaction with the mammalian immune system. The molecular basis of these attributes remains poorly understood, although candidate-based studies have implicated a handful of *Coccidioides* genes in growth and virulence.

Coccidioides is one of a group of thermally dimorphic fungal pathogens that grow in a sporulating hyphal form in the soil [3]. Upon introduction into the mammalian host, spores undergo differentiation into a parasitic form. Indeed, the defining characteristic of *Coccidioides* pathogenesis is development of the spore (arthroconidium) into a multicellular structure called the spherule [1,4]. In spherule development, instead of germinating and growing as polar hyphae, the arthroconidium undergoes isotropic enlargement in the mammalian lung with multiple rounds of mitosis prior to formation of internal spores (endospores) resulting in a 60 to 100 µm micron multi-cellular spherule, encased by a spherule outer wall [5]. If a spherule ruptures, endospores are released and can re-initiate the spherule cycle, either locally or following dissemination to other sites within the host. Known virulence genes in *Coccidioides* are expressed concomitant with spherule development [6–9]. One critical unanswered question in *Coccidioides* biology is the nature of the regulatory network that drives spherulation and virulence.

To identify putative regulators of spherulation, we assessed the role of the conserved fungal transcription factor, Ryp1, that is involved in development of the parasitic form in response to temperature for the other thermally dimorphic fungi. We had previously shown that the WOPR transcription factor Ryp1 is a master regulator that is required for the formation of the host form in the thermally dimorphic fungal pathogen *Histoplasma* [10,11]. Additionally, Ryp1 is a master regulator of gene expression in response to temperature in *Histoplasma*, as it is required for the vast majority of the gene expression program at 37ºC [10,11]. Investigating the role of Ryp1 in *Coccidioides* was particularly compelling since Ryp1 orthologs are found throughout the fungal kingdom and are required for key developmental transitions in numerous fungi [12–16]. For example, the *Candida albicans* ortholog Wor1 regulates cell-type specification by driving the switch from “white” cells to “opaque” cells [17,18].

Here we deleted the *RYP1* gene in *Coccidioides posadasii* and showed that the resultant mutant is unable to undergo mature spherulation. We used RNA-seq to show that Ryp1 has a

role in gene expression in both spherules and hyphae. The Δ*ryp1* mutant failed to express the normal complement of hypha-enriched transcripts, and most notably, the immature Δ*ryp1* spherules expressed only a subset of normal spherule-enriched genes, consistent with their inability to fully differentiate. The Δ*ryp1* mutant was completely avirulent in the mouse model of *Coccidioides* infection, demonstrating that the Ryp1 transcription factor is a key regulator that links the ability to form mature spherules and the expression of critical virulence traits.

Results

Deletion of *Coccidioides posadasii RYP1*

To define potential regulators of *Coccidioides* parasitic phase development, we identified the *C. posadasii* ortholog of the conserved regulator of fungal development, *RYP1,* based on similarity to the *H. capsulatum* Ryp1 protein [10]. Ryp1 is a member of the WOPR family of transcription factors. The *C. posadasii* strain Silveira *RYP1* gene, CPSG_00528, encodes a 404 amino acid protein that is 68% similar to the 487 *H. capsulatum RYP1* protein [10], with 84% identity and 91% similarity over the N-terminal half of the protein including the WOPRa and WOPRb regions and the putative nuclear localization signal). To determine the role of *RYP1* in the *C. posadasii* life cycle, gene replacement strains were made via *Agrobacterium* transformation [19,20]. Transformed lines were screened for homologous recombination of a deletion construct where the *E. coli hphB* gene was cloned between 1.2 kb 5' and 3' flanking regions of the *RYP1* gene, using an approach similar to that used for creation of the Δ*cps1* strain [19]. A total of 40 transformed lines were generated between two transformations with 42% being *RYP1* gene replacements as analyzed by DNA hybridization for the first set of transformants and PCR for the second set (data not shown). The *RYP1* gene replacement strains (Δ*ryp1*) have a single insertion of the 1.4 kb *E. coli hphB* expression cassette replacing the full 1.3 kb *RYP1* coding region. Phenotypic analyses of Δ*ryp1* mutants were performed using several independent transformed

121 strains and compared to the parental Silveira strain (WT) and one strain (1563.19) where the
122 *RYP1* deletion construct had integrated randomly in the genome leaving the *RYP1* gene intact.

123 **Ryp1 is required for *Coccidioides* development**

124 Deletion of *RYP1* resulted in several *in vitro* phenotypes (Fig 1). The Δ*ryp1* arthroconidia
125 were delayed in germination, with visible colonies appearing after 7 days at 25°C on 2X GYE
126 media while the progenitor WT and the ectopic transformed strains gave visible colonies three
127 days after plating. The radial growth of Δ*ryp1* colonies was also retarded relative to WT or ectopic
128 transformed strains (Fig 1G) and Δ*ryp1* colonies failed to grow to the edge of petri dishes (Fig 1A-
129 D). The Δ*ryp1* strains exhibited a granular phenotype at the edges of the colony (Fig 1E and F),
130 possibly indicative of more dense conidiation. The most dramatic phenotype was observed under
131 *in vitro* spherulation conditions: the Δ*ryp1* mutant failed to differentiate into mature spherules.
132 Instead the arthroconidia remained as thin-walled structures at all time points and by 72 hours
133 had formed short hyphal-like segmented structures (Fig 2).

134 **Figure 1**. **Growth morphology of Δ*ryp1* mutants**. *C. posadasii* Δ*ryp1* strains exhibit a
135 growth-limiting phenotype (A, C), in comparison to WT (B) and an ectopic transformant
136 (D). (E) The Δ*ryp1* strains have a granular phenotype. (F) Enlarged view of the Δ*ryp1*
137 colony edge is shown. (A-F) All colonies were inoculated at the center of the agar media
138 and grown at room temperature for 28 days. Representative image of each strain is shown.
139 (G) Plugs of 6 mm were transferred from freshly growing plates to 2X GYE plates and
140 incubated at room temperature, to measure colony radial growth. Colony diameters were
141 measured on days 8, 14 and 20. Four independent Δ*ryp1* strains (1563.4, 1563.6, 1563.7
142 and 1563.14), as well as the WT parental strain and an ectopic transformed strain (1563.1)
143 were tested.

144

145 **Figure 2: *C. posadasii* Δ*ryp1* does not produce normal spherules *in vitro*.** Spherules
146 of WT, a Δ*ryp1* mutant and an ectopic transformed strain, grown in Converse medium at

147 37°C with 20% CO_2 and aliquots analyzed during *in vitro* spherulation. Images at 24 h
148 show that while the WT and ectopic strains are rounding up to form early spherules, Δ*ryp1*
149 does not form round structures. At 96 h and 120 h, the WT and ectopic strains produced
150 mature spherules, while the Δ*ryp1* exhibited limited polar hyphal growth. Black bars
151 represent 10 μm.

152 **Ryp1 regulates distinct sets of genes in spherules and hyphae**

153 Our previous studies revealed that *H. capsulatum* Ryp1 is required for yeast-phase growth
154 and is responsible for the expression of the majority of yeast-phase specific genes *[10]*. Given
155 that *C. posadasii* Δ*ryp1* mutants are defective in spherulation, we postulated that *C. posadasii*
156 Ryp1 is also responsible for transcriptional regulation of morphology-associated genes. To this
157 end, we performed RNA-seq to transcriptionally profile WT and Δ*ryp1* strains of *C. posadasii*
158 grown under either spherulation or hyphal conditions. Under our experimental conditions, 9711
159 transcripts were observable (transcripts per million, TPM, ≥ 10) in at least one sample. Of these,
160 4175 transcripts (about 43% of all detected transcripts) were significantly differentially expressed
161 (Fig 3) with at least a two-fold change in at least one of the following three comparisons: (1) a
162 comparison of WT spherules and WT hyphae (WT^{Sph}/WT^{Hy}) identified 2985 transcripts that we
163 refer to as "morphology-regulated" genes; (2) a comparison of WT vs Δ*ryp1* under spherule
164 conditions identified 1742 Ryp1-dependent transcripts; and (3) a comparison of WT vs. Δ*ryp1*
165 under hyphal conditions identified 925 Ryp1-dependent transcripts (Fig 3B). Not all of these Ryp-1
166 dependent transcripts in comparisons 2 and 3 are morphology-regulated genes, and in fact, 1157
167 morphology-regulated transcripts (39% of the 2985 WT^{Sph}/WT^{Hy} comparison) were dependent on
168 Ryp1 either under spherulation or hyphal conditions. Thus, in contrast to *H. capsulatum*, over half
169 of the morphology-regulated expression is Ryp1-independent, and Ryp1 regulates distinct sets of
170 genes whose expression correlates with either spherule or hyphal growth conditions. To further
171 explore the 4175 differentially expressed transcripts, we grouped them in 17 classes by

expression pattern (Fig 3A, S1 Table). Ryp1-dependent transcription under spherulation conditions is correlated with WT morphology-regulated transcription: spherule-enriched genes are more likely to be Ryp1-induced (class 2 in Fig 3A) while hypha-enriched genes are more likely to be Ryp1-repressed in spherules (Fig 3C and class 4 in Fig 3A). In contrast, Ryp1-dependent transcription under hyphal conditions is not correlated with morphology-regulated transcription, as can be seen from the shape of the scatter plot (Fig 3D).

Figure 3. Ryp1 regulates distinct sets of genes in spherules and hyphae. (A) Heatmap showing differential expression of the 4175 genes described in the text. Genes are grouped by expression pattern (significantly up, down, or neutral in each of the three contrasts) with different classes labeled in the color bar to the right of the heatmap. The position of genes of interest in the heatmap are indicated to the right of the color bar. (B) Venn diagram of genes observed to be morphology-regulated (differentially expressed in WT^{Sph}/WT^{Hy}), Ryp1-dependent in spherulation conditions (differentially expressed in $WT^{Sph}/\Delta ryp1^{Sph}$), or Ryp1-dependent in hyphal conditions (differentially expressed in $WT^{Hy}/\Delta ryp1^{Hy}$). (C and D) Scatter plots of the differentially expressed genes comparing the WT spherule-enrichment (right) or hyphal-enrichment (left) to *ryp1*-depletion (top) or *ryp1*-enrichment (bottom) in (C) spherules or (D) hyphae. Genes in the scatter plots are colored by expression pattern, as in the color bar of (A).

Ryp1 is required for the expression of a set of spherule-enriched transcripts

Early subtractive cDNA hybridization experiments identified four spherule-specific genes (*ALD1*, *OPS1*, *PSP1*, and *MDR1*) [21]. Of these, we found that *ALD1* is spherule-enriched and Ryp1-independent (S1 Table, class 1) while the remaining three are both spherule-enriched and Ryp1-dependent at 37°C (S1 Table, class 2). Altogether, 406 (25%) of the 1593 transcripts that are more highly expressed in wild-type spherules versus hyphae are dependent on Ryp1 for their expression. This set includes SOWgp, the best characterized *Coccidioides* virulence factor [22]

and CPSG_05265 (CIMG_00509), a previously noted spherule enriched gene [6] at the boundary of a region of introgression between *C. immitis* and *C. posadasii* [23].

Intriguingly, about 5% (84 of 1593) of the spherule-enriched transcripts are more highly expressed in the Δ*ryp1* mutant than WT under spherulation conditions, (S1 Table, class 3), indicating their expression is normally repressed by Ryp1 in wild-type spherules. This set includes the sulfur assimilation pathway (*MET3*, *MET14*, *MET16*, and *MET10*) required to reduce intracellular sulfate to sulfide. In contrast, we found that the downstream genes *MET5* (the beta subunit to *MET10*) and *MET17A* (which catalyzes the first step of cysteine and methionine biosynthesis) are both spherule-enriched but Ryp1-independent, while the genes acting in opposition to sulfur assimilation (both the sulfite oxidase *SOX1* and the sulfite exporter *SSU1*) are spherule-enriched and Ryp1-dependent. These data are consistent with Ryp1 regulation promoting sulfur efflux versus influx.

Ryp1 regulates the expression of a set of hypha-enriched transcripts

Analysis of the hypha-enriched transcripts showed that about 25% of this set (351 out of 1392) are Ryp1-repressed when cells are grown under spherulation conditions (S1 Table, class 4). Notably, this set includes the APSES transcription factor *STU1*, which regulates hyphal morphology in *Histoplasma* [24] and has conserved hyphal enrichment in *C. immitis* [8] and all of the thermally dimorphic pezizomycetes for which RNA-seq data is available [25]. Additional genes in this set consistent with hyphal growth include 5 septins (*CDC10*, *CDC12*, *CDC3*, *ASPA*, and *ASPE*), which are cytoskeletal proteins involved in cell cycle regulation [26]. Intriguingly, 33 of the 351 genes in this set are also Ryp1-dependent under hyphal growth conditions. In particular, the *Coccidioides* ortholog of the OefC transcription factor, which confers a “fluffy” phenotype in *Aspergillus nidulans* when overexpressed [27], exhibits this Ryp1-dependent regulation in hyphae. Furthermore, about 12% (164 of the 1392) of the hypha-enriched transcripts are found to be Ryp1-dependent under hyphal-promoting conditions (S1 Table, class 5). This set includes the stress response gene *DDR48*/*MS95*, which is highly enriched in *Histoplasma* hyphae [28], as well as

both *DIT2*, an enzyme involved in the production of N,N-bisformyl dityrosine, and the bisformyl dityrosine transporter *DTR1*. In *Saccharomyces cerevisiae*, bisformyl dityrosine is a major building block of the protective ascospore cell wall, whose assembly depends on both *DIT2* [29] and *DTR1* [30]. These Ryp1-dependent hypha-enriched genes also include many enzymes with NADH cofactors, including two (CodA and AifA) with roles in the response to reductive stress [31,32]. Taken together, our results suggest that Ryp1 has a dual role in *Coccidioides* development, regulating the expression of subsets of both spherule- and hypha-enriched genes.

Ryp1 regulates expression of morphology- or temperature-independent transcripts

In *Histoplasma*, Ryp1 directly interacts with two other transcriptional regulators, Ryp2 and Ryp3, to regulate yeast-phase growth [11]. The orthologs of *RYP2* and *RYP3* in *Coccidioides* are not differentially regulated in wild-type spherules and hyphae; however, *RYP2* displays a Ryp1-dependent expression pattern under spherulation conditions (S1 Table, class 6). In addition, 282 transcripts show a similar morphology-independent but Ryp1-dependent expression pattern under spherulation conditions, including the cytosolic catalase *CATP*, the tyrosinase *TYR2*, as well as ~40 genes involved in primary carbohydrate, nucleotide, and amino acid metabolism. An additional 75 transcripts display a morphology-independent but Ryp1-dependent expression pattern under both spherule- and hypha-promoting conditions (S1 Table, class 7). Among these genes are *MEP1*, a protease that contributes to immune evasion via degradation of SOWgp [33]; urease (CPSG_08438), a known virulence factor of *Coccidioides [34]*; *UAZ1*, a uricase that catalyzes the first step in the breakdown of uric acid; and *CTR2*, a copper transporter observed to be spherule-enriched in *C. immitis*.

In addition to the Ryp1-dependent transcripts, there are 432 transcripts that are equivalently expressed in WT spherules and hyphae but are upregulated in Δ*ryp1* mutants compared to wild-type under spherulation conditions (S1 Table, class 8), suggesting that Ryp1 represses their expression. This set includes *LAE1*, a master regulator of secondary metabolism [35]; orthologs of the *Aspergillus* developmental regulators NsdD (*NSD4*) and FlbC (*FBC1*); the

MAPK pathway components *STE11*, *PBS2*, and *SDP1*; and the histidine kinase PhkB (*PHK2*). In *Histoplasma*, *PHKB* shares a Ryp1-associated divergent promoter with the histidine kinase *PHKA*, and both genes are Ryp1-induced in *Histoplasma* yeast [11]. In *Coccidioides*, these genes likewise share a divergent promoter, and have correlated expression profiles, but the differential expression of *PHKA* is too modest to pass our 2-fold change criterion.

A significant portion of the morphology-regulated genes are expressed independently of Ryp1

In addition to the spherule-enriched genes that were regulated by Ryp1, there was a significant portion of spherule-enriched genes that were independent of Ryp1. In fact, of 1593 transcripts that are upregulated in wild-type spherules compared to hyphae, 62% of them (1002 transcripts) show Ryp1-independent expression patterns (S1 Table, class 1). Notably, these include genes involved in regulation of morphology: *XBP1*, an APSES transcription factor enriched in *Histoplasma* yeast [24], *SSK1* and *SKN7*, response regulators required for *Histoplasma* yeast morphology (Beyhan et al, unpublished), the redox related genes *TSA1* and *NIR1*, and *HPD1*, which has previously been noted as a morphology related gene in *Coccidioides* [6,9] and *Paracoccidioides* [36]. Similarly, among 1392 hypha-enriched transcripts, 62% (862 transcripts) are Ryp1-independent in our dataset (S1 Table, class 9). These include five enzymes of gluconeogenesis (*PCK1*, *GAPDH (TDH1)*, *TPI1*, and *FBP1*), as well as genes related in glutamate import, amino acid catabolism, peptidase activity, and protein complex disassembly -- all consistent with hyphae utilizing proteins as a primary carbon source. Notably, *PYC2*, the first enzyme of gluconeogenesis, is both enriched in hyphae and Ryp1-repressed in spherules.

***RYP1* deletion mutants are avirulent**

The critical role of Ryp1 in spherule formation and gene regulation suggested that it may be either reduced in virulence, or avirulent, *in vivo*. To test this, we assessed the virulence of the Δ*ryp1* strain using the mouse model of coccidioidomycosis in C57BL/6 mice. Twelve mice were intranasally infected with 50 or 1,000 arthroconidia of Δ*ryp1* strain 1563.7 and disease

progression was compared to infection with 50 WT arthroconidia or 4,400 Δ*cps1* spores which were previously shown to be avirulent [19]. Fungal burden in the lungs and spleen as well as survival was monitored for 28 days post-infection. Additionally, two mice from each group were sacrificed after 12 days for histopathological studies. The WT-infected mice all became moribund and were euthanized between day 12 and 19, while all Δ*ryp1* and Δ*cps1*-infected mice survived to day 28. Lung and spleen homogenates did not yield *Coccidioides* colony-forming units (CFUs) from infections with the Δ*ryp1* and Δ*cps1* mice, consistent with an inability of these mutant strains to survive *in vivo*. In a follow-up experiment, four additional Δ*ryp1* strains were screened for virulence along with an ectopic transformed line (Fig 4). As in the first experiment, Δ*ryp1*-infected mice, which received between 525 and 1133 arthroconidia, survived for the full duration of the 28-day study (Fig 4). In contrast, seven of eight mice infected with 52 spores of the ectopically integrated *RYP1* deletion construct or infected with 49 WT spores died by day 17. One mouse in each of these two groups survived for 28 days but had significant pulmonary disease and dissemination and would have ultimately succumbed to the infection. As we observed previously, there was no growth of *Coccidioides* from the lungs or spleens of the Δ*ryp1*-infected mice. The mean lung CFUs of the mice infected with ectopic strain 1563.1 were 2.87×10^7 (range 1.24×10^5- 4.7×10^7), and for those infected with WT were 1.31×10^7 (range 1.06×10^5 – 4.8×10^7), with dissemination to the spleens in all mice as reflected by spleen CFUs.

Figure 4: Infection of mice with *C. posadasii* Δ*ryp1*. Survival results for C57BL/6 mice (N=8 mice/group) infected intranasally with four independent Δ*ryp1* strains, 1563.7 (circle), 1563.10 (square), 1563.14 (inverted triangle) and 1563.15 (triangle), one ectopic *ryp1*-transformed strain, 1563.1 (half-filled circle) and WT (half-filled square). The Δ*ryp1* strains were infected at between 525 and 1133 arthroconidia, while 50 arthroconidia of the ectopic stain and WT were used.

Δ*ryp1* mutants do not provide protection against WT infection

Due to the failure of Δ*ryp1* to cause disease or persist in the lungs of C57BL/6 mice, the Δ*ryp1* strain was tested to determine whether it provides protective immunity against subsequent WT infection, as is the case for the Δ*cps1* strain. The Δ*cps1* vaccine strain and the Δ*ryp1* strain 1563.7 were used to vaccinate C57BL/6 mice either intraperitoneally (IP) or subcutaneously (SC) as described previously [19]. Mice were vaccinated, boosted after two weeks, challenged four weeks later with 90 WT arthroconidia, and sacrificed two weeks later. While Δ*cps1* provided dramatic protection by either SC or IP vaccination, resulting in a 5-log lower lung fungal burden than mice vaccinated with a control adjuvant, vaccination with Δ*ryp1* resulted in no reduction in lung fungal burden and thus, no protection (Fig 5). Mice in the control group had a mean lung fungal burden of 5.3 x 10^6 CFU, which was similar to that of the Δ*ryp1* SC-vaccinated mice ($P<0.05$) which had mean lung fungal burdens of 4.1 x 10^6 CFU and the Δ*ryp1* IP-vaccinated mice with an average of 6.4 x 10^6 CFU per lung. In contrast, the Δ*cps1*-vaccinated mice had mean lung fungal burdens of 341 CFU for the IP-vaccinated group and 84 CFU for the SC-vaccinated group. -Furthermore, when whole spleens were plated for fungal growth, those from Δ*cps1-v*-accinated mice were almost fully free of fungi, with only one spleen of a single Δ*cps1* IP-vaccinated mouse having a small area of growth, likely from a single spherule, appearing seven days after plating, while the control mice and Δ*ryp1*--vaccinated mice all grew *Coccidioides* by three days after plating. Thus it is clear that the Δ*ryp1* strain does not provide protective immunity against *Coccidioides* infection.

Figure 5: Vaccination of mice with *C. posadasii* Δ*ryp1* mutant. Protection results for C57BL/6 mice vaccinated with either Δ*cps1,* Δ*ryp1* or a *S. cerevisiae* culture supernatant (Control). C57BL/6 mice (N=8 mice/group) were injected either by intraperitoneal (IP) or subcutaneous (SC) injection twice 2 weeks apart with Δ*cps1,* Δ*ryp1*, or Control. Vaccinated mice were challenged with a lethal dose of WT (90 spores) and total lung CFUs were determined 14 days post-infection. Δ*cps1* significantly protects mice from *C.*

posadasii infection compared to Control (P<0.004 both comparisons) while Δ*ryp1* shows no protection (P=0.99 vs. control). Bar equals geometric mean.

Discussion

Spherulation is a critical step of pathogenesis in *Coccidioides* infection, allowing the fungus to adapt to growth within the host and producing endospores which allow expansion and dissemination of the fungus. Here we identified the first transcription factor that is essential for the process of *Coccidioides* spherulation by interrogating the function of Ryp1, a conserved transcriptional regulator that plays a critical role in fungal development and virulence in many fungi, including *Histoplasma*, a close relative of *Coccidioides*. Our results showed that as in *Histoplasma*, Ryp1 is required for development of the host parasitic form; namely spherules in *Coccidioides* and yeast-phase cells in *Histoplasma*. Additionally, in *Coccidioides*, we demonstrated that Ryp1 is absolutely required for virulence in the mouse model of infection, consistent with its critical role in spherulation. The Δ*ryp1* strain failed to differentiate into spherules *in vitro* and failed to persist in susceptible B6 mice, producing no symptoms of disease or viable propagules at 28 days post-infection, even when exposed to 10-20X the level of spores that results in a lethal infection for WT strains. Interestingly, in contrast to *Histoplasma*, where Ryp1 is required for the differential expression of the vast majority of yeast-enriched transcripts, there were a significant number of spherule-enriched genes whose expression was Ryp1-independent, indicating that other transcription factors likely function in parallel to Ryp1 to regulate spherule development. Additionally, *Coccidioides* Ryp1 is required for normal rates of radial growth of hyphal colonies and regulates the expression of a subset of hypha-enriched transcripts. Thus *Coccidioides* Ryp1 has a dual role in both the environmental form and the host form of the fungus where it regulates gene expression and development.

The contrast between *Histoplasma* and *Coccidioides* Ryp1 should be interpreted in the light of the evolutionary relationship between *Histoplasma* and *Coccidioides*--although both are thermally dimorphic fungal pathogens in the order Onygenales, *Histoplasma* is a member of the

family Ajellomycetaceae, which also includes the thermally dimorphic pathogens *Paracoccidioides, Blastomyces,* and *Emergomyces*, consistent with a single origin of dimorphism in this family. In contrast, *Coccidioides* is the only known dimorphic member of the family Onygenaceae, and has a unique dimorphic pattern, forming endosporulating spherules during host invasion vs. the more typical hyphal to yeast phase transition. This evolutionary relationship suggests that dimorphism of *Histoplasma* and *Coccidioides* evolved separately, and that some regulatory mechanisms may be shared whereas others are distinct. In *Histoplasma*, since Ryp1 is required for the vast majority of yeast-enriched expression, identifying Ryp-dependent genes by expression analysis of WT vs *ryp1* mutants did not further refine the set of yeast-enriched transcripts defined by comparing the gene expression program of wild-type *Histoplasma* yeast and hyphae [10]. In contrast, only 25% of spherule-enriched transcripts were dependent on *Coccidioides* Ryp1, thereby suggesting that these genes may be key to spherule development and virulence, both of which are defective in the absence of Ryp1. Further identification of key effectors of *Coccidioides* spherulation and virulence could come from future studies identifying direct targets of Ryp1, which was useful in identifying virulence factors in *Histoplasma [11]*.

Transcriptome differences between *Coccidioides* spherules and hyphae have previously been profiled using RNA-seq in both *C. posadasii* and *C. immitis [6,8,37]*. In our dataset, about 30% of the detectable transcripts were differentially regulated between *C. posadasii* spherules and hypha. While there is not a complete overlap with other studies, likely due to differences in growth conditions and stage of spherule development, most of the previously observed highly regulated genes are also differentially regulated in our dataset. For example, SOWgp, the best characterized virulence factor of *Coccidioides* [22], is spherule-enriched in all datasets, and we observe its expression to be Ryp1-dependent. Among the shared hypha-enriched genes in all datasets, *STU1*, an APSES transcription factor that is a regulator of hyphal growth in *Histoplasma [24]*, is Ryp1-repressed in spherules, underscoring the importance of Ryp1 for the expression of morphology-specific genes.

SOWgp, one of the most highly enriched spherule-specific transcripts, is an important component of the *Coccidioides* spherule outer wall (SOW) layer [22]. This lipid-rich layer shed by spherules has been shown to reduce fungicidal activity of neutrophils towards arthroconidia and to promote disseminated disease [38]. The SOW lipids are composed of phospholipids and sphingolipids, with the major sphingolipids being sphingosine and ceramide [38]. In this study, we found that PilA and NCE102, two key factors for assembling eisosomes, punctate membrane associated structures involved in regulating lipid metabolism in response to stress, are enriched in spherules in a Ryp1-dependent manner. Given that eisosomes have a positive role in regulating sphingolipid synthesis [39], and that CPSG_03079, which is orthologous to the ceramide synthase BarA [40], is likewise spherule-enriched and Ryp1-dependent, it is plausible that Ryp1 may regulate production of SOW lipids in spherules.

The transcriptome profiling presented here showed that Ryp1 is responsible for inducing the expression of some spherule-enriched genes and repressing the expression of some hypha-enriched genes. Intriguingly, in addition to these sets of genes, there are other sets of spherule-enriched genes that are not regulated by Ryp1 under spherulation conditions, but are regulated by Ryp1 under hypha-promoting conditions. For example, *RYP4*, which is a major regulator of yeast growth in *Histoplasma*, is only regulated by Ryp1 under hyphal conditions. Here we found that *RYP4* is spherule-enriched in *C. posadasii*, as was also shown in *C. immitis* [8]. However, unlike *Histoplasma*, where *RYP4* expression under yeast-promoting conditions is directly regulated by Ryp1 [11], *RYP4* expression is independent of Ryp1 under spherulation conditions, but dependent on Ryp1 under hyphal conditions (S1 Table, class 10). An additional 67 genes share this expression pattern, including *ACH1*, which is required for detoxification of acetate in *S. cerevisiae* [43] and propionate in *A. fumigatus* [44]. Coexpression of *RYP4* and *ACH1* is notable, given the role of the *RYP4* ortholog FacB in regulation of acetate metabolism in *Aspergillus* [45].

403 The potential role of Ryp4 in regulating acetate utilization or morphological transitions in
404 *Coccidioides* will be determined by future studies.

405 In this study, we also explored the role of Ryp1 in pathogenesis using the murine model
406 of coccidioidomycosis. Our results show that Ryp1 is essential for *in vivo* growth and colonization;
407 however, it does not confer protection to the host, unlike the previously characterized Δ*cps1*
408 mutant. Intriguingly, the Δ*cps1* mutant is able to convert to spherules but is impaired in
409 development of mature spherules and endospores [19], whereas the morphology of the Δ*ryp1*
410 mutant *in vivo* is not yet known. Given its morphology defect *in vitro*, we predict that the Δ*ryp1*
411 mutant may not be able to convert to spherules *in vivo*, and thus may not display spherule-specific
412 antigens that are required to elicit a protective host response. Consequently, comparison of the
413 Δ*ryp1* and Δ*cps1* mutants may narrow the search for the molecules responsible for the protective
414 effect of the Δ*cps1* mutant. Furthermore, while the Δ*ryp1* mutant may not be a good vaccine
415 candidate, Ryp1 and other proteins that are required for spherule growth may be effective targets
416 for the development of therapeutics that inhibit the transition from arthroconidia to spherules *in*
417 *vivo*. Additionally, elucidation of the Ryp1 regulon as described here identifies key downstream
418 effectors that are essential for the development and virulence of the host form of *Coccidioides*,
419 and thus also serve as valuable diagnostic and therapeutic targets.

420

421 **Materials and Methods**

422 **Strains and growth conditions**

423 Wild-type *Coccidioides posadasii* (strain Silveira, ATCC 28868) was cultured on 2X GYE medium
424 (2% glucose, 1% yeast extract, and 1.5% agar) at room temperature (approximately 24°C).
425 Mutant strains were selected and maintained on 2X GYE media supplemented with 50 mg/ml of
426 hygromycin, also at room temperature as described previously [19]. Arthroconidia of WT and
427 mutant strains were harvested from 4 week-old cultures, using sterile water by the mini-stir bar
428 method described previously [46] and stored in sterile water at 4°C. Spore numbers were

429 determined with a hemocytometer and viable counts by serial dilution and plating. All
430 manipulations of viable cultures were performed at biosafety level 3 (BSL3). Spherules were
431 prepared by growth in a modified Converse medium at 38°C with 20% CO_2, with shaking at 180
432 rpm for 48 hours. To measure colonial radial growth and assess colony morphology, 6 mm plugs
433 of actively growing cultures were transferred to 2X GYE agar plates using transfertubes
434 (Transfertube® Disposable Harvesters, Spectrum® Laboratories,) and grown at room temperature.

435 **Creation of *RYP1* gene deletion mutants**

436 A gene replacement cassette for the *C. posadasii* strain Silveira *RYP1* gene (CPSG_00528) was
437 constructed using double-joint PCR [47]. DNA fragments of 1.2kb (5' 1192 and 3' 1233)
438 representing the 5' and 3'flanking sequences of CPSG_00528 were amplified by PCR with
439 oligonucleotide primer combinations OAM1153/OAM1154, and OAM1155/OAM1156,
440 respectively (Table S3). The hygromycin resistance gene (*E. coli hphB*) was amplified with
441 primers OAM597/OAM598. These three amplicons were then recombined by double-joint PCR
442 as described [47]. The extension product was amplified by PCR with the nested primers
443 OAM1159/OAM1160 which contain *Bam*HI restriction sites added at the ends. This product was
444 cloned into pGEM®-T Easy (Promega) and the insert in plasmid AM1538 was sequenced to verify
445 the construct. The gene replacement cassette was cloned as a *Bam*HI fragment into AM1145,
446 the binary vector for *Agrobacterium tumefaciens* transformation [48], creating AM1563. AM1563
447 was transformed into *A. tumefaciens* strain AD965. *C. posadasii* strain Silveira was transformed
448 with AD965/AM1563 as previously described [48] and hygromycin resistant strains selected and
449 passaged three times to get homokaryons, prior to molecular analysis. Gene replacement strains
450 and ectopic insertion transformants were identified by Southern hybridization analysis as
451 described previously [48], or by PCR. For PCR analysis, primers OAM597 and OAM598 were
452 used to confirm the presence of the hphB gene in all transformants. Primers OAM1611 located
453 upstream of the *RYP1* locus and OAM431 of the *hphB* gene were used to detect a homologous
454 integration event of the transforming construct at the 5' end of *RYP1*, and primers OAM1612

455 located downstream of the *RYP1* locus along with OAM432 were used to detect homologous
456 integration of the transforming construct at the 3' end of *RYP1*. For initial experiments including
457 *in vitro* growth, Δ*ryp1* strains 1563.1, 1563.4, 1563.7 and 1563.14 were used along with ectopic
458 transformed line 1563.19, where the *RYP1* deletion construct was integrated elsewhere in the
459 genome. For mouse virulence and protection studies, Δ*ryp1* strain 1563.7 was used. For further
460 experiments to validate mouse virulence results, an additional set of strains were used; Δ*ryp1*
461 strains 1563.7, 1563.10, 1563.14 and 1563.15 and ectopic transformed strain 1563.1.

462 **RNA-seq library preparation and sequencing**

463 For expression studies, total RNAs were isolated from WT and Δ*ryp1* hyphal and spherule
464 cultures. Duplicate hyphal cultures of each strain were grown by inoculation of 5 x 10^7
465 arthroconidia into 100 ml of 2X GYE and then incubated with shaking at 180 rpm for 48 h at 28°C.
466 Spherule cultures of WT and Δ*ryp1* were also grown in duplicate by inoculating 100 ml of modified
467 Converse liquid medium with 3 x 10^8 arthroconidia and growing them at 38°C with 20% CO_2, with
468 shaking at 180 rpm for 48 h [49]. RNAs were isolated using a modified acid-phenol preparation
469 as described previously [49] with the modification that liquid N_2 grinding was used to initially
470 disrupt the cells. RNAs were resuspended in diethyl pyrocarbonate-treated dH_2O prior to
471 assessment of their quality and concentration with an Agilent Bioanalyzer (Agilent Technologies,
472 Palo Alto, CA).

473 RNA-seq libraries were prepared as previously described [25]. Briefly, for the isolation of
474 mRNAs, five µg total RNA from each sample was subjected to poly-A purification using
475 Dynabeads Oligo $(dT)_{25}$(Invitrogen-ThermoFisher). RNA libraries were prepared using NEBNext
476 Ultra Directional RNA Library Prep Kit (NEB). Quality of the total RNA, mRNA and library was
477 confirmed using Bioanalyzer (Agilent). Sequencing was done in-house at UCSF Center for
478 Advanced Technology using Illumina HiSeq2500 instruments. 11 to 19 million single-end 50 bp
479 reads were obtained for each sample.

480

RNA-seq data analysis

Predicted mRNA sequences for *Coccidioides posadasii* Silveira were downloaded from the Broad Institute on 3/18/2015 (http://www.broadinstitute.org/annotation/genome/coccidioides_group/MultiDownloads.html) [23,50].

Relative abundances (reported as TPM values [51]) and estimated counts (est_counts) of each transcript in each sample were estimated by alignment free comparison of k-mers between the preprocessed reads and mRNA sequences using KALLISTO version 0.46.0 [52]. Further analysis was restricted to transcripts with TPM ≥ 10 in at least one sample.

Differentially expressed genes were identified by comparing replicate means for contrasts of interest using LIMMA version 3.30.8 [53,54]. Genes were considered significantly differentially expressed if they were statistically significant (at 5% FDR) with an effect size of at least 2x (absolute log2 fold change ≥ 1) for a given contrast.

Murine virulence and protection studies

To assess the pathogenicity of Δ*ryp1* mutants, 8-week old female C57BL/6 mice (B6) were anesthetized with ketamine/xylazine and infected intranasally (IN) as previously described [55]. Briefly, 8-10 mice per group were challenged with 50 or 1000 spores of the Δ*ryp1* mutant strains. As a control, B6 mice were given 50 WT spores, and in some studies, B6 mice were infected with 50 spores of a transformed line with an ectopic insertion of the *RYP1* gene deletion construct.

The potential for Δ*ryp1* strains to protect mice from subsequent infection by WT was assessed by performing vaccination experiments as described for Δ*cps1* [19]. Six-week old B6 mice were primed with 2.5 x 10^4 Δ*ryp1* (strain 1563.7) arthroconidia either by intraperitoneal (IP) or subcutaneous (SC) injection of spores in groups of eight mice and two weeks later boosted

with the same number of spores. Two other groups of mice were used as a positive control for vaccination by being vaccinated in a similar manner with Δ*cps1* arthroconidia, at a dose of 5 x 10^4 spores. As a control, mice were vaccinated with a *S. cerevisiae* culture supernatant, which was previously used as an adjuvant for a chimeric protein antigen that shows some vaccine protection for *Coccidioides* [56]. Mice were challenged four weeks later with 90 WT arthroconidia and sacrificed two weeks later for lung fungal burden determination. Spleens were cultured whole to determine dissemination [56]. All murine infections and handling were carried out at animal BSL3 facility and all procedures with mice were approved by the University of Arizona Institutional Animal Care and Use Committee. Animals were housed and cared for according to PHS standards.

Other software and libraries

We wrote custom scripts and generated plots in Prism (GraphPad Software, San Diego, CA), R 3.3.3 [57] and Python 2.7.13, using Numpy 1.12.1 [58] and Matplotlib 2.0.0 [59]. Jupyter 4.2.3 [60] notebooks and JavaTreeView 1.1.6r4 [61] were used for interactive data exploration.

Data Availability

All relevant data are contained within the paper and/or Supporting Information files. For high-throughput sequencing data, the raw data are available at the NCBI Gene Expression Omnibus (GEO) databases under GEO accession GSE178277.

Supporting Data

S1 Table. Table of Kallisto quantification, limma statistics, and annotations for differentially expressed genes. Excel-compatible tab-delimited text conforming to JavaTreeView extended CDT format. Each row is a transcript with the UNIQID column giving the Broad Cp Silveira systematic gene name. The NAME column gives manually curated short gene names, transferred from *Histoplasma capsulatum* G217B (HcG217B, GenBank GCA_017607445.1) augmented with *Coccidioides*-specific gene names. The next three columns

give limma BH-adjusted p-values for differential expression in each of the three contrasts. The next 8 columns give kallisto estimated counts for each sample. The next 8 columns give kallisto normalized abundances (TPMs) for each sample. Cp_GenBank and Cp_anno give the GenBank Cp Silveira accession and annotation respectively. CiRS, CiRS_GenBank, and Ci_anno give the Broad systematic gene name, GenBank accession, and annotation respectively for the InParanoid-mapped *C. immitis* RS ortholog. HcG217B, HcG217B_anno, and HcG217B_GenBank give the GSC systematic gene name and annotation (from Voorhies et al, submitted) and GenBank accession for the InParanoid-mapped HcG217B ortholog. Cp_new_GenBank gives the GenBank accession for the corresponding gene in the newly available Cp Silveira assembly and annotation (BioProject PRJNA664774) [62]. Class indicates the differential expression pattern, as referenced in the results and discussion sections. BGCOLOR gives the hex code for the class coloring in Fig 3. GWEIGHT is a place-holder column for JavaTreeView compatibility. The final three columns give the limma fit values for the three contrasts plotted in Fig 3.

S2 Table. Table of Kallisto quantification, limma statistics, and annotations for all expressed genes. Excel-compatible tab-delimited text conforming to JavaTreeView extended CDT format. Columns are exactly as for S1 Table, but rows include all 9711 analyzed genes. The estimated counts in this file are sufficient to recapitulate the limma analysis.

S3 Table. Table of oligonucleotides used for Δ*ryp1* mutant creation and analysis.

Acknowledgements: We thank members of the Beyhan, Galgiani, Orbach, and Sil labs for helpful discussions.

553

554 **References**

555 1. Johnson L, Gaab EM, Sanchez J, Bui PQ, Nobile CJ, Hoyer KK, et al. Valley fever: danger
556 lurking in a dust cloud. Microbes Infect. 2014;16: 591–600.

557 2. Centers for Disease Control and Prevention (CDC). Increase in reported
558 coccidioidomycosis--United States, 1998-2011. MMWR Morb Mortal Wkly Rep. 2013;62:
559 217–221.

560 3. Sil A, Andrianopoulos A. Thermally Dimorphic Human Fungal Pathogens--Polyphyletic
561 Pathogens with a Convergent Pathogenicity Trait. Cold Spring Harb Perspect Med. 2014;5:
562 a019794.

563 4. Cole GT, Sun SH. Arthroconidium-Spherule-Endospore Transformation in Coccidioides
564 immitis. Fungal Dimorphism. 1985. pp. 281–333. doi:10.1007/978-1-4684-4982-2_12

565 5. Cole GT, Hung CY. The parasitic cell wall of Coccidioides immitis. Med Mycol. 2001;39
566 Suppl 1: 31–40.

567 6. Whiston E, Zhang Wise H, Sharpton TJ, Jui G, Cole GT, Taylor JW. Comparative
568 transcriptomics of the saprobic and parasitic growth phases in Coccidioides spp. PLoS
569 One. 2012;7: e41034.

570 7. Johannesson H, Kasuga T, Schaller RA, Good B, Gardner MJ, Townsend JP, et al. Phase-
571 specific gene expression underlying morphological adaptations of the dimorphic human
572 pathogenic fungus, Coccidioides posadasii. Fungal Genet Biol. 2006;43: 545–559.

573 8. Carlin AF, Beyhan S, Peña JF, Stajich JE, Viriyakosol S, Fierer J, et al. Transcriptional
574 Analysis of Coccidioides immitis Mycelia and Spherules by RNA Sequencing. Journal of

Fungi. 2021. doi:10.3390/jof7050366

9. Viriyakosol S, Singhania A, Fierer J, Goldberg J, Kirkland TN, Woelk CH. Gene expression in human fungal pathogen Coccidioides immitis changes as arthroconidia differentiate into spherules and mature. BMC Microbiol. 2013;13: 1–1.

10. Nguyen VQ, Sil A. Temperature-induced switch to the pathogenic yeast form of Histoplasma capsulatum requires Ryp1, a conserved transcriptional regulator. Proceedings of the National Academy of Sciences. 2008;105: 4880.

11. Beyhan S, Gutierrez M, Voorhies M, Sil A. A Temperature-Responsive Network Links Cell Shape and Virulence Traits in a Primary Fungal Pathogen. PLoS Biol. 2013;11: e1001614.

12. Lohse MB, Zordan RE, Cain CW, Johnson AD. Distinct class of DNA-binding domains is exemplified by a master regulator of phenotypic switching in Candida albicans. Proc Natl Acad Sci U S A. 2010;107: 14105–14110.

13. Michielse CB, Becker M, Heller J, Moraga J, Collado IG, Tudzynski P. The Botrytis cinerea Reg1 protein, a putative transcriptional regulator, is required for pathogenicity, conidiogenesis, and the production of secondary metabolites. Mol Plant Microbe Interact. 2011;24: 1074–1085.

14. Jonkers W, Dong Y, Broz K, Kistler HC. The Wor1-like protein Fgp1 regulates pathogenicity, toxin synthesis and reproduction in the phytopathogenic fungus Fusarium graminearum. PLoS Pathog. 2012;8: e1002724.

15. Brown DW, Busman M, Proctor RH. Fusarium verticillioides SGE1 is required for full virulence and regulates expression of protein effector and secondary metabolite biosynthetic genes. Mol Plant Microbe Interact. 2014;27: 809–823.

16. Michielse CB, van Wijk R, Reijnen L, Manders EMM, Boas S, Olivain C, et al. The nuclear protein Sge1 of Fusarium oxysporum is required for parasitic growth. PLoS Pathog. 2009;5: e1000637.

17. Srikantha T, Borneman AR, Daniels KJ, Pujol C, Wu W, Seringhaus MR, et al. TOS9 regulates white-opaque switching in Candida albicans. Eukaryot Cell. 2006;5: 1674–1687.

18. Zordan RE, Galgoczy DJ, Johnson AD. Epigenetic properties of white–opaque switching in Candida albicans are based on a self-sustaining transcriptional feedback loop. Proceedings of the National Academy of Sciences. 2006;103: 12807.

19. Narra HP, Shubitz LF, Mandel MA, Trinh HT, Griffin K, Buntzman AS, et al. A Coccidioides posadasii CPS1 Deletion Mutant Is Avirulent and Protects Mice from Lethal Infection. Infect Immun. 2016;84: 3007–3016.

20. Abuodeh RO, Orbach MJ, Mandel MA, Das A, Galgiani JN. Genetic transformation of Coccidioides immitis facilitated by Agrobacterium tumefaciens. J Infect Dis. 2000;181: 2106–2110.

21. Delgado N, Hung CY, Tarcha E, Gardner MJ, Cole GT. Profiling gene expression in Coccidioides posadasii. Med Mycol. 2004;42: 59–71.

22. Hung C-Y, Yu J-J, Seshan KR, Reichard U, Cole GT. A parasitic phase-specific adhesin of Coccidioides immitis contributes to the virulence of this respiratory Fungal pathogen. Infect Immun. 2002;70: 3443–3456.

23. Neafsey DE, Barker BM, Sharpton TJ, Stajich JE, Park DJ, Whiston E, et al. Population genomic sequencing of Coccidioides fungi reveals recent hybridization and transposon control. Genome Res. 2010;20: 938–946.

619 24. Longo LVG, Ray SC, Puccia R, Rappleye CA. Characterization of the APSES-family
620 transcriptional regulators of Histoplasma capsulatum. FEMS Yeast Res. 2018;18: 991.

621 25. Rodriguez L, Voorhies M, Gilmore S, Beyhan S, Myint A, Sil A. Opposing signaling
622 pathways regulate morphology in response to temperature in the fungal pathogen
623 Histoplasma capsulatum. PLoS Biol. 2019;17: e3000168.

624 26. Gladfelter AS. Control of filamentous fungal cell shape by septins and formins. Nat Rev
625 Microbiol. 2006;4: 223–229.

626 27. Lee B-Y, Han S-Y, Choi HG, Kim JH, Han K-H, Han D-M. Screening of growth- or
627 development-related genes by using genomic library with inducible promoter in Aspergillus
628 nidulans. J Microbiol. 2005;43: 523–528.

629 28. Gilmore SA, Voorhies M, Gebhart D, Sil A. Genome-Wide Reprogramming of Transcript
630 Architecture by Temperature Specifies the Developmental States of the Human Pathogen
631 Histoplasma. PLoS Genet. 2015;11: e1005395.

632 29. Briza P, Eckerstorfer M, Breitenbach M. The sporulation-specific enzymes encoded by the
633 DIT1 and DIT2 genes catalyze a two-step reaction leading to a soluble LL-dityrosine-
634 containing precursor of the yeast spore wall. Proc Natl Acad Sci U S A. 1994;91: 4524–
635 4528.

636 30. Felder T, Bogengruber E, Tenreiro S, Ellinger A, Sá-Correia I, Briza P. Dtrlp, a multidrug
637 resistance transporter of the major facilitator superfamily, plays an essential role in spore
638 wall maturation in Saccharomyces cerevisiae. Eukaryot Cell. 2002;1: 799–810.

639 31. Thön M, Al Abdallah Q, Hortschansky P, Scharf DH, Eisendle M, Haas H, et al. The
640 CCAAT-binding complex coordinates the oxidative stress response in eukaryotes. Nucleic
641 Acids Res. 2010;38: 1098–1113.

642 32. Savoldi M, Malavazi I, Soriani FM, Capellaro JL, Kitamoto K, da Silva Ferreira ME, et al.
643 Farnesol induces the transcriptional accumulation of the Aspergillus nidulans Apoptosis-
644 Inducing Factor (AIF)-like mitochondrial oxidoreductase. Mol Microbiol. 2008;70: 44–59.

645 33. Hung C-Y, Seshan KR, Yu J-J, Schaller R, Xue J, Basrur V, et al. A metalloproteinase of
646 Coccidioides posadasii contributes to evasion of host detection. Infect Immun. 2005;73:
647 6689–6703.

648 34. Mirbod-Donovan F, Schaller R, Hung C-Y, Xue J, Reichard U, Cole GT. Urease produced
649 by Coccidioides posadasii contributes to the virulence of this respiratory pathogen. Infect
650 Immun. 2006;74: 504–515.

651 35. Bayram O, Braus GH. Coordination of secondary metabolism and development in fungi: the
652 velvet family of regulatory proteins. FEMS Microbiol Rev. 2012;36: 1–24.

653 36. Nunes LR, Costa de Oliveira R, Leite DB, da Silva VS, dos Reis Marques E, da Silva
654 Ferreira ME, et al. Transcriptome analysis of Paracoccidioides brasiliensis cells undergoing
655 mycelium-to-yeast transition. Eukaryot Cell. 2005;4: 2115–2128.

656 37. Mead HL, Roe CC, Higgins Keppler EA, Van Dyke MCC, Laux KL, Funke AL, et al.
657 Defining Critical Genes During Spherule Remodeling and Endospore Development in the
658 Fungal Pathogen, Coccidioides posadasii. Front Genet. 2020;11: 483.

659 38. Peláez-Jaramillo CA, Jiménez-Alzate MDP, Araque-Marin P, Hung C-Y, Castro-Lopez N,
660 Cole GT. Lipid Secretion by Parasitic Cells of Contributes to Disseminated Disease. Front
661 Cell Infect Microbiol. 2021;11: 592826.

662 39. Lanze CE, Gandra RM, Foderaro JE, Swenson KA, Douglas LM, Konopka JB. Plasma
663 Membrane MCC/Eisosome Domains Promote Stress Resistance in Fungi. Microbiol Mol
664 Biol Rev. 2020;84. doi:10.1128/MMBR.00063-19

665 40. Li S, Du L, Yuen G, Harris SD. Distinct ceramide synthases regulate polarized growth in the
666 filamentous fungus Aspergillus nidulans. Mol Biol Cell. 2006;17: 1218–1227.

667 41. Hwang LH, Mayfield JA, Rine J, Sil A. Histoplasma requires SID1, a member of an iron-
668 regulated siderophore gene cluster, for host colonization. PLoS Pathog. 2008;4: e1000044.

669 42. Yuan WM, Gentil GD, Budde AD, Leong SA. Characterization of the Ustilago maydis sid2
670 gene, encoding a multidomain peptide synthetase in the ferrichrome biosynthetic gene
671 cluster. J Bacteriol. 2001;183: 4040–4051.

672 43. Fleck CB, Brock M. Re-characterisation of Saccharomyces cerevisiae Ach1p: fungal CoA-
673 transferases are involved in acetic acid detoxification. Fungal Genet Biol. 2009;46: 473–
674 485.

675 44. Fleck CB, Brock M. Characterization of an acyl-CoA: carboxylate CoA-transferase from
676 Aspergillus nidulans involved in propionyl-CoA detoxification. Mol Microbiol. 2008;68: 642–
677 656.

678 45. Todd RB, Kelly JM, Davis MA, Hynes MJ. Molecular characterization of mutants of the
679 acetate regulatory gene facB of Aspergillus nidulans. Fungal Genet Biol. 1997;22: 92–102.

680 46. Huppert M, Sun SH, Gross AJ. Evaluation of an experimental animal model for testing
681 antifungal substances. Antimicrob Agents Chemother. 1972;1: 367–372.

682 47. Yu J-H, Hamari Z, Han K-H, Seo J-A, Reyes-Domínguez Y, Scazzocchio C. Double-joint
683 PCR: a PCR-based molecular tool for gene manipulations in filamentous fungi. Fungal
684 Genet Biol. 2004;41: 973–981.

685 48. Kellner EM, Orsborn KI, Siegel EM, Mandel MA, Orbach MJ, Galgiani JN. Coccidioides
686 posadasii contains a single 1,3-beta-glucan synthase gene that appears to be essential for

687 growth. Eukaryot Cell. 2005;4: 111–120.

688 49. Mandel MA, Galgiani JN, Kroken S, Orbach MJ. Coccidioides posadasii contains single
689 chitin synthase genes corresponding to classes I to VII. Fungal Genet Biol. 2006;43: 775–
690 788.

691 50. Sharpton TJ, Stajich JE, Rounsley SD, Gardner MJ, Wortman JR, Jordar VS, et al.
692 Comparative genomic analyses of the human fungal pathogens Coccidioides and their
693 relatives. Genome Res. 2009;19: 1722–1731.

694 51. Li B, Dewey CN. RSEM: accurate transcript quantification from RNA-Seq data with or
695 without a reference genome. BMC Bioinformatics. 2011;12: 323.

696 52. Bray NL, Pimentel H, Melsted P, Pachter L. Near-optimal probabilistic RNA-seq
697 quantification. Nat Biotechnol. 2016;34: 525–527.

698 53. Ritchie ME, Phipson B, Wu D, Hu Y, Law CW, Shi W, et al. limma powers differential
699 expression analyses for RNA-sequencing and microarray studies. Nucleic Acids Res.
700 2015;43: e47.

701 54. Smyth GK. Linear models and empirical bayes methods for assessing differential
702 expression in microarray experiments. Stat Appl Genet Mol Biol. 2004;3: Article3.

703 55. Shubitz L, Peng T, Perrill R, Simons J, Orsborn K, Galgiani JN. Protection of mice against
704 Coccidioides immitis intranasal infection by vaccination with recombinant antigen 2/PRA.
705 Infect Immun. 2002;70: 3287–3289.

706 56. Shubitz LF, Yu J-J, Hung C-Y, Kirkland TN, Peng T, Perrill R, et al. Improved protection of
707 mice against lethal respiratory infection with Coccidioides posadasii using two recombinant
708 antigens expressed as a single protein. Vaccine. 2006;24: 5904–5911.

57. R Core Team. R: A language and environment for statistical computing, v3.3.3. R Foundation for Statistical Computing, Vienna, Austria. 2021 [cited 2021]. Available: https://www.r-project.org/

58. van der Walt S, Colbert SC, Varoquaux G. The NumPy Array: A Structure for Efficient Numerical Computation. Computing in Science Engineering. 2011;13: 22–30.

59. Hunter. Matplotlib: A 2D Graphics Environment. Computing in Science & Engineering. 2007;9: 90–95.

60. Perez F, Granger BE. IPython: A System for Interactive Scientific Computing. Computing in Science Engineering. 2007;9: 21–29.

61. Saldanha AJ. Java Treeview--extensible visualization of microarray data. Bioinformatics. 2004;20: 3246–3248.

62. de Melo Teixeira M, Stajich JE, Sahl JW, Thompson GR, Blackmon AV, Mead HL, et al. A chromosomal-level reference genome of the widely utilized Coccidioides posadasii laboratory strain “Silveira.” bioRxiv. 2021. p. 2021.05.19.444813. doi:10.1101/2021.05.19.444813

Mandel et al. Figure 1

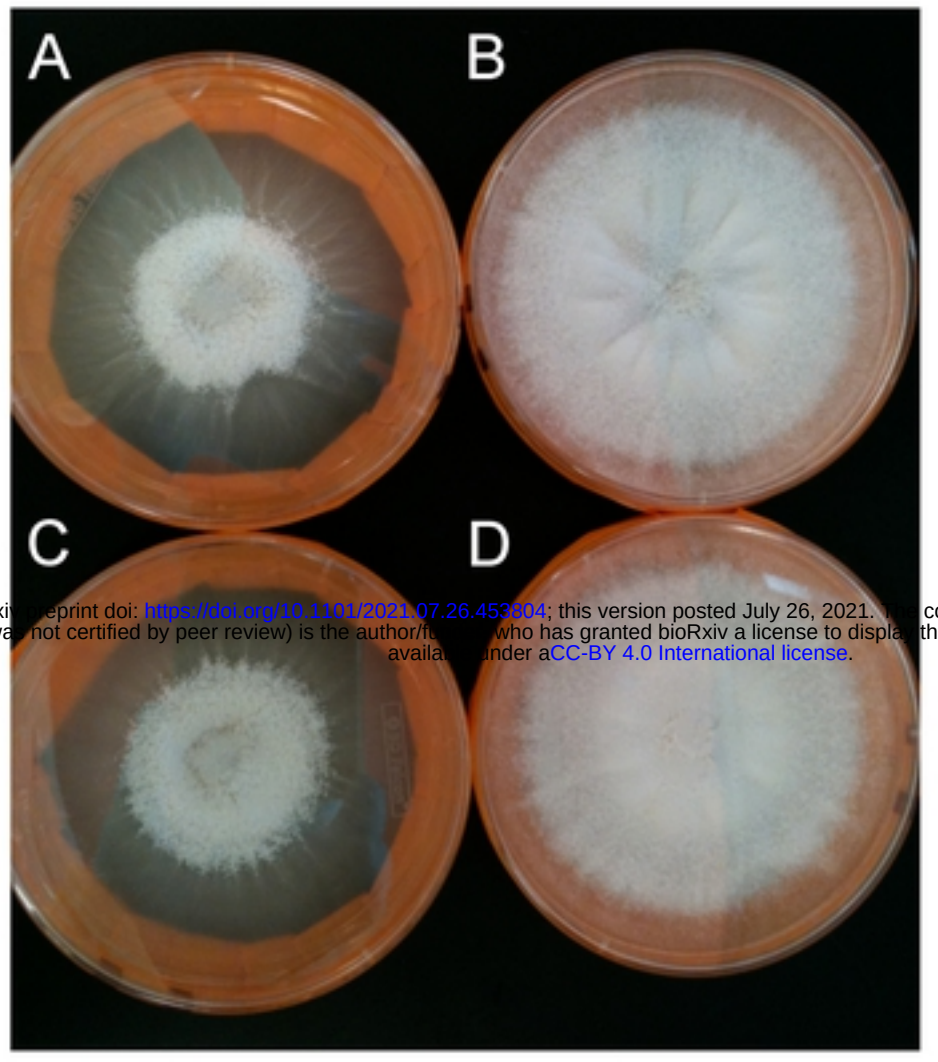

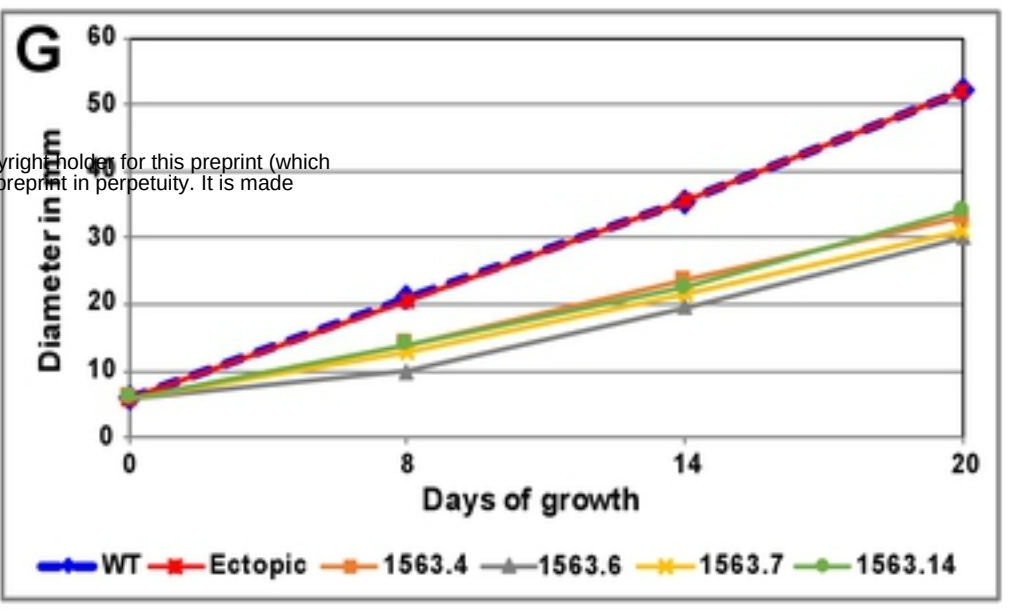

Mandel et al. Figure 2

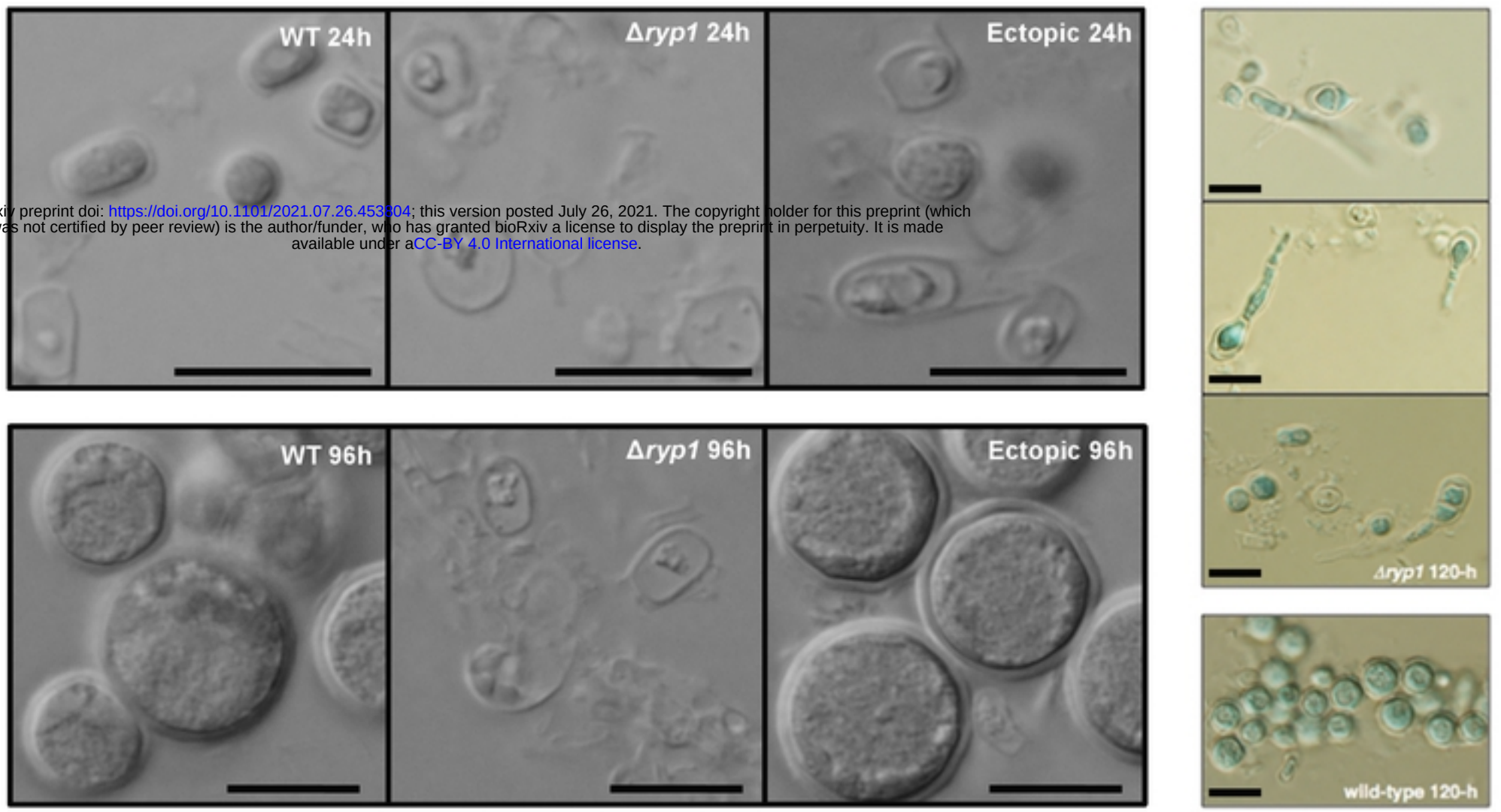

Mandel et al. Figure 3

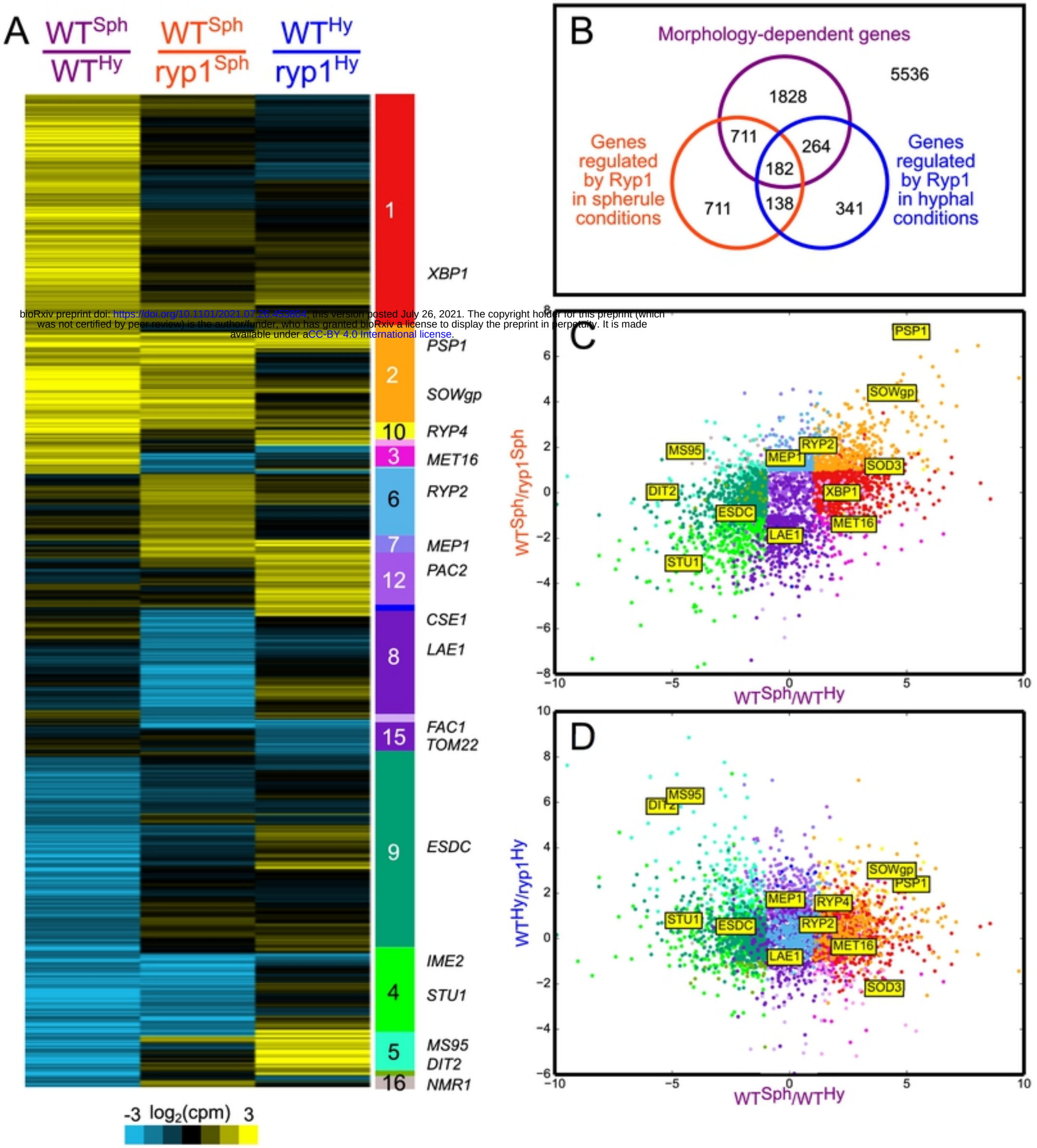

Mandel et al. Figure 4

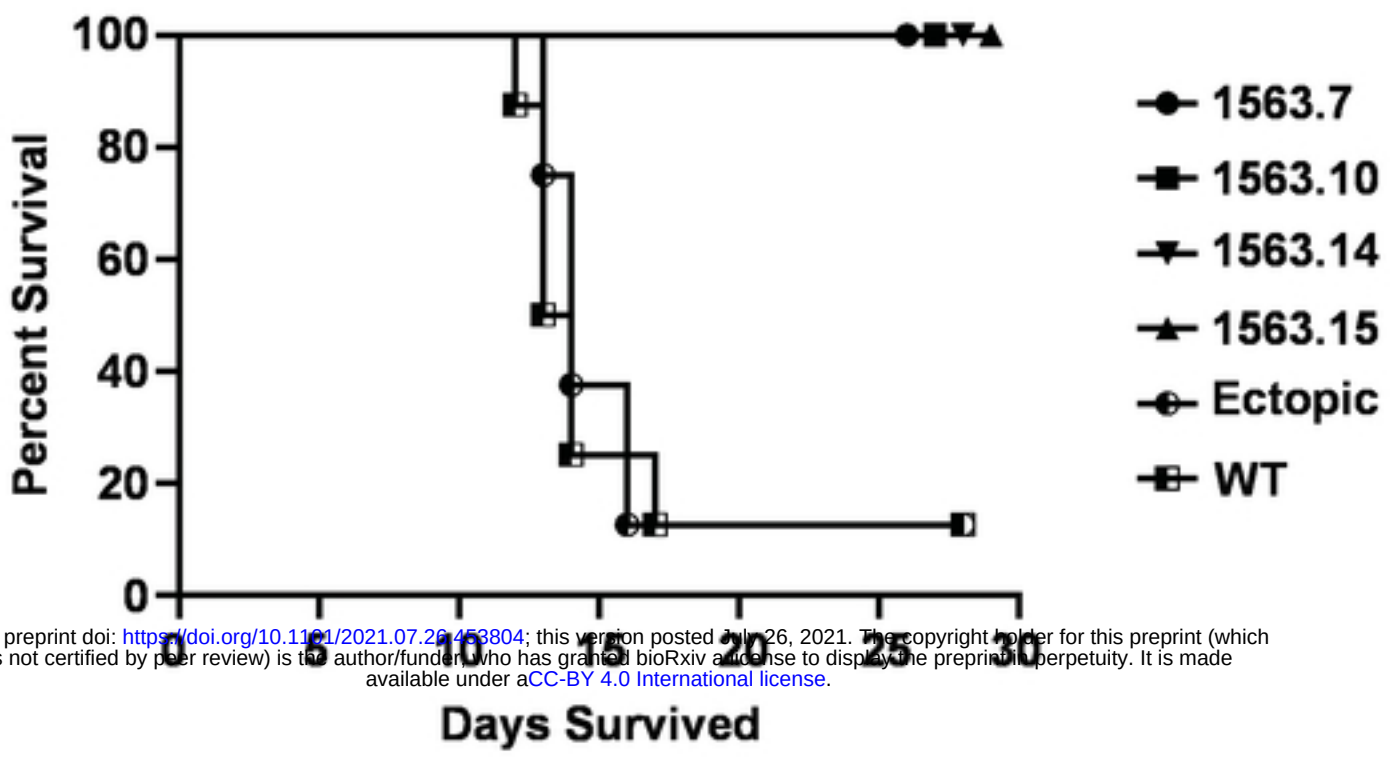

Mandel et al. Figure 5